LA-UR-16-20704 (Accepted Manuscript)

Bounded extremum seeking with discontinuous dithers

Scheinker, Alexander
Scheinker, David

To be published in: Automatica

DOI to publisher's version: 10.1016/j.automatica.2016.02.023

Permalink to record: http://permalink.lanl.gov/object/view?what=info:lanl-repo/lareport/LA-UR-16-20704

Bounded Extremum Seeking with Discontinuous Dithers ⋆

Alexander Scheinker [a], David Scheinker [b],

[a] *Los Alamos National Laboratory, Los Alamos, New Mexico, USA*

[b] *Massachusetts Institute of Technology, Cambridge, Massachusetts, USA*

Abstract

The analysis of discontinuous extremum seeking (ES) controllers, e.g. those applicable to digital systems, has historically been more complicated than that of continuous controllers. We establish a simple and general extension of a recently developed bounded form of ES to a general class of oscillatory functions, including functions discontinuous with respect to time, such as triangle or square waves with dead time. We establish our main results by combining a novel idea for oscillatory control with an extension of functional analytic techniques originally utilized by Kurzweil, Jarnik, Sussmann, and Liu in the late 80s and early 90s and recently studied by Dürr et al. We demonstrate the value of the result with an application to inverter switching control.

Key words: Extremum Seeking; Stabilization; Unknown Systems

1 Introduction

Classical Extremum Seeking Optimization (ESO) began in the 1920s, using a slowly oscillating perturbation to guide a system's output to an extremum value [1]. A series of papers in the 50s and 60s [2–6], were the first analytic studies of the stability of ESO. These results were refined and expanded to a wider class of systems in [7–12].

This form of ESO has been used in many applications [13] with unknown/uncertain systems [14] and with discontinuous sliding-mode type ES perturbations [15]. Furthermore, ESO has been used for applications such as active flow control [16,17], aeropropulsion [18], cooling systems [19], wind energy [20], photovoltaics [21], electromagnetic valve actuation [22], human exercise machines [23], enhancing mixing in magnetohydrodynamic channel flows [24], controlling Tokamak plasmas [25], and recently, utilizing a multivariable Newton-based ESO scheme, for the power optimization of photovoltaic micro-converters [26] as well as Newton-based stochastic extremum seeking [27].

In [28] a new form of Extremum Seeking Control and Optimization (ESCO) was introduced which, unlike ESO, is applicable to unstable and time-varying systems and utilizes the extremum seeker as the feedback controller itself. ESCO is closely related to the field of vibrational control and highly oscillatory systems [29–36]. Whereas ESO has been used to optimize the output of a-priori stable, controlled systems, ESCO can be used to control and optimize uncertain, time-varying, open-loop unstable systems.

Since its inception ESCO has been used to optimize a high voltage converter modulator [37]; to stabilize and expand the region of attraction of a pendulum's vertical equilibrium point [38]; it has been studied on manifolds [39]; a non-differentiable form of ESCO was developed in which the system's control efforts settle to zero as equilibrium is approached [40]; and a bounded form of ESCO was developed for unknown and possibly open-loop unstable systems in which the control efforts and parameter update rates have analytically known bounds [41], and implemented in hardware to tune a particle accelerator based only on an extremely noisy measurement signal [42].

Our main result, Theorem 1, extends the study of bounded ESCO from smoothly varying sinusoidal functions, to a much larger useful class of not necessarily continuous functions, e.g., a perturbing signal common in digital systems, a square wave with dead time between pulses. Theorem 1 has four useful properties:

⋆ This research was supported by Los Alamos National Laboratory and the Massachusetts Institute of Technology. This paper was not presented at any IFAC meeting. Corresponding author A. Scheinker. Tel. +1914-582-0932.

Email addresses: ascheink@lanl.gov (Alexander Scheinker), dscheink@mit.edu (David Scheinker).

(1) It establishes feedback control that is, on average, immune to additive, state-independent measurement noise.
(2) It is applicable to time-varying nonlinear systems.
(3) It establishes the on-average equivalence of variety of control choices that may be used with a range of different types of hardware.
(4) The proof is simpler and the result more general than the related work in [29–33].

2 Main Theoretical Result

We use the notation $u(y,t) = u(\hat{\psi}(x,t),t)$ to emphasize that the controller need not have direct access to x, i.e., that u is a function of t and of a noise corrupted measurement of a potentially unknown function $\hat{\psi}(x,t) = \psi(x,t) + n(t)$. We recall that a sequence of functions $\{f_k\} \subset L^2[0,1]$ is said to converge weakly to f in $L^2[0,1]$, denoted $f_k \rightharpoonup f$, if

$$\lim_{k\to\infty} < f_k, g >= \lim_{k\to\infty} \int_0^1 f_k(\tau)g(\tau)d\tau$$
$$= \int_0^1 f(\tau)g(\tau)d\tau =< f, g >, \quad \forall g \in L^2[0,1].$$

Our primary result is the following.

Theorem 1 *Consider the vector-valued system*

$$\dot{x} = f(x,t) + g(x,t)u(y,t), \tag{1}$$
$$y = \psi(x,t) + n(t) = \hat{\psi}(x,t), \tag{2}$$

where $x \in \mathbb{R}^n$, and the functions $f : \mathbb{R}^n \times \mathbb{R} \to \mathbb{R}^n$, $g : \mathbb{R}^n \times \mathbb{R} \to \mathbb{R}^{n\times n}$, $\psi : \mathbb{R}^n \times \mathbb{R} \to \mathbb{R}$, and $n(t) : \mathbb{R} \to \mathbb{R}$ are unknown and twice continuously differentiable with respect to x. Also, ψ and $\partial\psi/\partial t$ are bounded with respect to t for x in a compact set, and $n(t), \dot{n}(t)$ are bounded. Consider a controller $u : \mathbb{R} \times \mathbb{R} \to \mathbb{R}^n$, given by

$$u(y,t) = \sum_{i=1}^{m} k_i(y,t)h_{i,\omega}(t), \quad k_i : \mathbb{R} \times \mathbb{R} \to \mathbb{R}^n, \tag{3}$$

where the functions $k_i(y,t)$ are continuously differentiable and the functions $h_{i,\omega}(t)$ are piece-wise continuous. System (1) - (3) has the following equivalent closed-loop form

$$\dot{x}(t) = f(x,t) + \sum_{i=1}^{m} b_i(x,t)h_{i,\omega}(t), \tag{4}$$
$$b_i(x,t) = g(x,t)k_i\left(\hat{\psi}(x,t),t\right). \tag{5}$$

Suppose that the integrals of the functions $h_{i,\omega}(t)$ satisfy the uniform limits

$$\lim_{\omega\to\infty} H_{i,\omega}(t) = \lim_{\omega\to\infty} \int_{t_0}^{t} h_{i,\omega}(\tau)d\tau = 0, \tag{6}$$

and the weak limits

$$h_{i,\omega}(t)H_{j,\omega}(t) \rightharpoonup \lambda_{i,j}(t). \tag{7}$$

Consider also the average system related to (1) - (3) as follows

$$\dot{\bar{x}} = f(\bar{x},t) - \sum_{i,j=1}^{n} \lambda_{i,j}(t)\frac{\partial b_i(\bar{x},t)}{\partial \bar{x}} b_j(\bar{x},t), \quad \bar{x}(0) = x(0). \tag{8}$$

For any compact set $K \subset \mathbb{R}^n$, any $t_0, T \in \mathbb{R}_{\geq 0}$, and any $\delta > 0$, there exists $\omega^\star$ such that for each $\omega > \omega^\star$, the trajectories $x(t)$ and $\bar{x}(t)$ of (4) and (8), satisfy

$$\max_{t\in[t_0,t_0+T]} \|x(t) - \bar{x}(t)\| < \delta. \tag{9}$$

Furthermore,

$$\lim_{t\to\infty} \|\bar{x}(t)\| = 0 \Longrightarrow \lim_{t\to\infty} \|x(t)\| < \delta.$$

In other words, uniform asymptotic stability of (8) over K implies the semiglobal practical uniform asymptotic stability of (1) - (3).

The proof and definitions are given in the Appendix.

A simple example of a system of form (1)-(3) will illustrate the consequences of the theorem using the controller that motivated this work.

Example 1 *Consider the system*

$$\dot{x} = ax + bu, \quad u = \sqrt{\alpha\omega}\cos\left(\omega t + kx^2\right) \tag{10}$$

noting that when the sign of b is unknown, one cannot design a classical PID type stabilizing controller. Theorem 1 implies that the closed loop average system related to (10) is given by

$$\dot{\bar{x}} = \left(a - k\alpha b^2\right)\bar{x}, \tag{11}$$

which is stabilized by a sufficiently large choice of $k\alpha > \frac{a}{b^2}$, regardless of the sign of b. We now provide the details of how Theorem 1 is applied, carrying out weak limit calculations which we will routinely omit in the remainder of the paper. In the notation used in Theorem 1, system

(10) may be written as

$$\dot{x} = \underbrace{ax}_{f(x)} + \underbrace{b}_{g(x)} u, \quad y = \underbrace{x}_{\psi(x)} \tag{12}$$

$$\begin{aligned} u &= \sqrt{\alpha\omega}\cos\left(\omega t + kx^2\right) \\ &= \underbrace{\sqrt{\alpha\omega}\cos\left(\omega t\right)}_{h_{1,\omega}(t)} \underbrace{\cos\left(kx^2\right)}_{k_1(x)} \underbrace{-\sqrt{\alpha\omega}\sin\left(\omega t\right)}_{h_{2,\omega}(t)} \underbrace{\sin\left(kx^2\right)}_{k_2(x)}, \end{aligned} \tag{13}$$

which has closed loop form

$$\begin{aligned} \dot{x} = ax &+ \underbrace{\sqrt{\alpha\omega}\cos\left(\omega t\right)}_{h_{1,\omega}(t)} \underbrace{b\cos\left(kx^2\right)}_{b_1(x)} \\ &\underbrace{-\sqrt{\alpha\omega}\sin\left(\omega t\right)}_{h_{2,\omega}(t)} \underbrace{b\sin\left(kx^2\right)}_{b_2(x)}. \end{aligned} \tag{14}$$

Consider the sequence of functions $\{h_{1,\omega}(t)\} = \{\sqrt{\alpha\omega}\cos(\omega t)\}$ *and* $\{h_{2,\omega}(t)\} = \{-\sqrt{\alpha\omega}\sin(\omega t)\}$ *where* $\omega \to \infty$. *Consider corresponding sequences* $\{H_{i,\omega}(t) = \int_0^t h_{i,\omega}(\tau)d\tau\}$ *where*

$$H_{1,\omega}(t) = \sqrt{\frac{\alpha}{\omega}}\sin\left(\omega(t)\right), \quad H_{2,\omega}(t) = \sqrt{\frac{\alpha}{\omega}}\cos\left(\omega(t)\right)$$

and notice that for each i, *the functions* $H_{i,\omega}(t)$ *converge uniformly to* 0 *as* $\omega \to \infty$. *In the present example, according the Riemann-Lebesgue Lemma [49],*

$$\begin{aligned} h_{1,\omega}(t)H_{1,\omega}(t) &= \alpha\cos\left(\omega t\right)\sin\left(\omega t\right) \rightharpoonup \lambda_{1,1} = 0 \\ h_{1,\omega}(t)H_{2,\omega}(t) &= \alpha\cos^2\left(\omega t\right) \rightharpoonup \lambda_{1,2} = \frac{\alpha}{2} \\ h_{2,\omega}(t)H_{1,\omega}(t) &= -\alpha\sin^2\left(\omega t\right) \rightharpoonup \lambda_{2,1} = -\frac{\alpha}{2} \\ h_{2,\omega}(t)H_{1,\omega}(t) &= -\alpha\sin\left(\omega t\right)\cos\left(\omega t\right) \rightharpoonup \lambda_{2,2} = 0. \end{aligned}$$

Therefore, according to Theorem 1, the average system is given by

$$\begin{aligned} \dot{\bar{x}} &= a\bar{x} + \frac{1}{2}\left(\frac{\partial b_1}{\partial \bar{x}} b_2 \lambda_{1,2} + \frac{\partial b_2}{\partial \bar{x}} b_1 \lambda_{2,1}\right) \\ &= \left(a - k\alpha b^2\right)\bar{x}. \end{aligned} \tag{15}$$

The stability of this system over compact sets implies the $\frac{1}{\omega}$ *- semiglobal practical uniform asymptotic stability of the original system (10).*

3 Immunity to measurement noise

An important noise-rejecting feature of the average system dynamics, (8), is buried in the partial derivative $\frac{\partial b_i(\bar{x},t)}{\partial \bar{x}}$. We illustrate this below.

Consider the problem of minimizing the unknown function $\psi(x,t)$ based only on a noise corrupted measurement, in a system of the form,

$$\dot{x} = b(t)u(y), \quad y = \hat{\psi}(x,t) = \psi(x,t) + n(t), \tag{16}$$

where $b(t)$ is an unknown, time-varying control direction. Consider a controller of the form,

$$u = h_{1,\omega}(t) + h_{2,\omega}(t)\hat{\psi}(x,t), \tag{17}$$

such that the functions $h_{i,\omega}(t)$ satisfy the assumptions of Theorem 1, with $\lambda_{1,2} = \lambda_{2,1} = 1$. In this case, relative to (8), $b_1(y,t) = b(t)$ and $b_2(y,t) = b(t)y$, and the average system dynamics are

$$\begin{aligned} \dot{\bar{x}} &= -b_2\frac{\partial b_1}{\partial \bar{x}} - b_1\frac{\partial b_2}{\partial \bar{x}}, \\ &= -b^2(t)\hat{\psi}(\bar{x},t)\frac{\partial}{\partial \bar{x}}\left(1\right) - b^2(t)\frac{\partial}{\partial \bar{x}}\left(\psi(\bar{x},t) + n(t)\right), \\ &= -b^2(t)\frac{\partial \psi(\bar{x},t)}{\partial \bar{x}}. \end{aligned} \tag{18}$$

Therefore, when $b(t)$ is not identically zero, the system, on average, converges towards a minimum of the actual function $\psi(x,t)$ despite having access only to its noise-corrupted measurement $\hat{\psi}(x,t)$.

Remark 1 *In practice, if there is any large noise in the system,* $n(t)$, *at a given frequency,* ω_0, *then the dithering frequency,* ω, *should be chosen such that* $\omega \neq \omega_0$, *this can always be done by choosing* $\omega > \omega_0$.

4 The on-average equivalence of various dithers

Different dithers are appropriate in different control designs. In an analog system based on sinusoidal oscillators, a sinusoidal dither is a natural choice. In a switching system, such as the high voltage application in Section 5, a square wave with dead time is the choice that can be implemented in hardware. Theorem 1 has the useful property that a variety of different controllers have, on average, identical dynamics. This is illustrated with the following simulation which extends the work in [43] to this new form of bounded ESCO, including discontinuous step-function dithers as were studied for ESO in [15].

Consider the linear system

$$\dot{x} = a_{11}x + a_{12}y + b_1 u_x(\psi(x,y),t), \tag{19}$$

$$\dot{y} = a_{21}x + a_{22}y + b_2 u_y(\psi(x,y),t), \tag{20}$$

where $\psi(x,y)$ is an analytically unknown function to be minimized. We will consider four controllers, one of which is a perturbing signal common in digital systems, a square wave with dead time between pulses. We pick

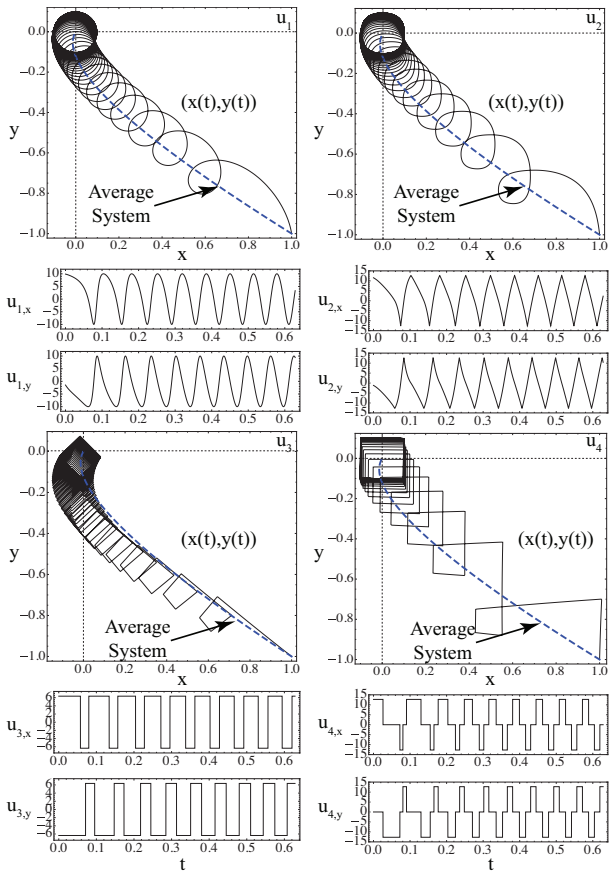

Fig. 1. The trajectories of system (19), (20) with controllers u_1, u_2, u_3, and u_4 are shown next to the trajectory of their common average system (38), (39). Control efforts in each case are shown for only a few of the initial oscillations in which the phase modulation is obvious.

gains such that the $\lambda_{i,j}$ equal $\pm\frac{1}{2}$ for all dither choices, which results in a uniform convergence rate for all controllers. As the averaged systems for each choice of dither are equivalent, so are their domains of attraction. The amplitude of the final, steady state oscillation about the stable equilibrium of the average system, is the same $\sqrt{\frac{\alpha}{\omega}}$ for each choice of dither.

The first controller is smooth, it is given by:

$$u_{1,x} = \cos\left(\omega t + k\psi(x,y)\right)\sqrt{\alpha\omega}, \tag{21}$$
$$u_{1,y} = \sin\left(\omega t + k\psi(x,y)\right)\sqrt{\alpha\omega}, \tag{22}$$

which can be expanded via trigonometric identities as

$$\begin{aligned} u_{1,x} = {} & \sqrt{\alpha\omega}\cos(\omega t)\cos(k\psi(x,y)) \\ & -\sqrt{\alpha\omega}\sin(\omega t)\sin(k\psi(x,y)), \end{aligned} \tag{23}$$
$$\begin{aligned} u_{2,x} = {} & \sqrt{\alpha\omega}\cos(\omega t)\sin(k\psi(x,y)) \\ & +\sqrt{\alpha\omega}\sin(\omega t)\cos(k\psi(x,y)), \end{aligned} \tag{24}$$

and then the overall dynamics can be rewritten as

$$\begin{aligned} \begin{bmatrix}\dot{x}\\ \dot{y}\end{bmatrix} = {} & \begin{bmatrix} a_{11} & a_{12}\\ a_{21} & a_{22}\end{bmatrix}\begin{bmatrix} x\\ y\end{bmatrix} \\ & + \underbrace{\sqrt{\omega}\cos(\omega t)}_{h_{1,\omega}(t)} \underbrace{\begin{bmatrix} b_1\sqrt{\alpha}\cos(k\psi(x,y))\\ b_2\sqrt{\alpha}\sin(k\psi(x,y))\end{bmatrix}}_{k_1(x,y)} \\ & + \underbrace{\sqrt{\omega}\sin(\omega t)}_{h_{2,\omega}(t)} \underbrace{\begin{bmatrix} -b_1\sqrt{\alpha}\sin(k\psi(x,y))\\ b_2\sqrt{\alpha}\cos(k\psi(x,y))\end{bmatrix}}_{k_2(x,y)}. \end{aligned} \tag{25}$$

The second controller is continuous, but not differentiable, and is implemented by the use of phase shifted triangle waves of period $\frac{2\pi}{\omega}$:

$$u_{2,x} = f_{\text{tri},1}\left(\omega t + k\psi(x,y)\right)\frac{4}{\pi}\sqrt{\alpha\omega}, \tag{26}$$
$$u_{2,y} = f_{\text{tri},2}\left(\omega t + k\psi(x,y)\right)\frac{4}{\pi}\sqrt{\alpha\omega}, \tag{27}$$

where $f_{\text{tri},1}(t)$ is in phase with $\cos(t)$ and $f_{\text{tri},2}(t)$ is in phase with $\sin(t)$. One particular, analytical form of such controllers is

$$u_{2,x} = \left(1 - 2\left\|f_{\text{tri}}\left[\cos\left(\omega\frac{t}{2} + k\frac{\psi(x,y)}{2}\right)\right]\right\|\right)\frac{4}{\pi}\sqrt{\alpha\omega}, \tag{28}$$
$$u_{2,y} = f_{\text{tri}}\left[\cos\left(\omega t + k\psi(x,y)\right)\right]\frac{4}{\pi}\sqrt{\alpha\omega}. \tag{29}$$

In this case the λ_{ij} are determined by integrals of triangle waves.

The third controller is given by the discontinuous square wave of period $\frac{2\pi}{\omega}$:

$$u_{3,x} = f_{\text{sqr},1}\left(\omega t + k\psi(x,y)\right)\frac{2}{\pi}\sqrt{\alpha\omega}, \tag{30}$$
$$u_{3,y} = f_{\text{sqr},2}\left(\omega t + k\psi(x,y)\right)\frac{2}{\pi}\sqrt{\alpha\omega}, \tag{31}$$

where $f_{\text{sqr},1}(t)$ is in phase with $\cos(t)$ and $f_{\text{sqr},2}(t)$ is in phase with $\sin(t)$. Which can be expressed as

$$u_{3,x} = \text{sgn}\left[\cos\left(\omega t + k\psi(x,y)\right)\right]\frac{2}{\pi}\sqrt{\alpha\omega}, \tag{32}$$
$$u_{3,y} = \text{sgn}\left[\sin\left(\omega t + k\psi(x,y)\right)\right]\frac{2}{\pi}\sqrt{\alpha\omega}. \tag{33}$$

In this case the λ_{ij} are determined by integrals of sign functions.

The last controller is the most realistic for digital implementation. Is is given by a square wave of period $\frac{2\pi}{\omega}$

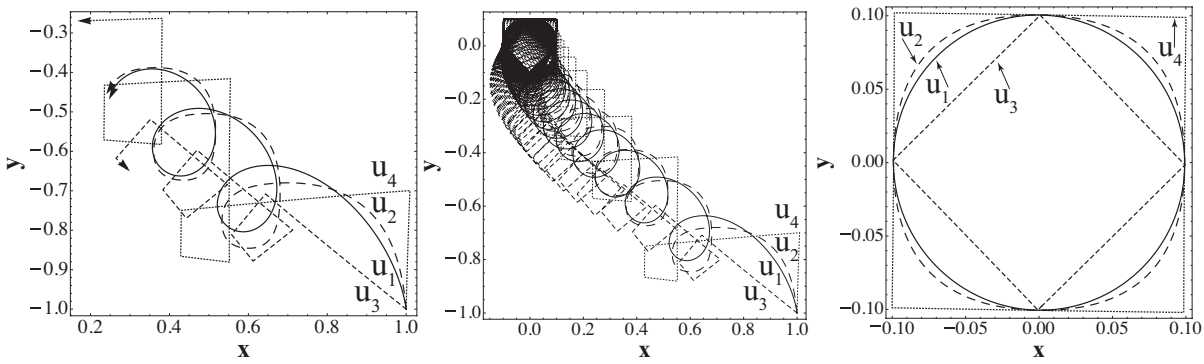

Fig. 2. **Left:** Initial $\frac{3.5\times 2\pi}{\omega}$ seconds of the simulation of system (19), (20), shows the various trajectories evolving with similar average velocities. **Center:** Evolution of the trajectories over the entire simulation time. **Right:** The last $\frac{2\pi}{\omega}$ seconds of the simulation, when all trajectories have settled near the origin, but in this case are slightly tilted due to the destabilizing terms a_{ij}. The size of the oscillation about the final point of convergence is given in each case by a circle (U_1), ellipse (u_2), diamond (u_3), and square (u_4) of size $\sqrt{\frac{\alpha}{\omega}} = \frac{1}{10}$ as analytically predicted by the choice of gains.

with dead time:

$$u_{4,x} = f_{\text{sqrd},1}\left(\omega t + k\psi(x,y)\right)\frac{2}{\pi}\sqrt{\alpha\omega}, \tag{34}$$

$$u_{4,y} = f_{\text{sqrd},1}\left(\omega t + k\psi(x,y)\right)\frac{2}{\pi}\sqrt{\alpha\omega}, \tag{35}$$

where $f_{\text{sqrd},1}(t)$ is in phase with $\cos(t)$ and $f_{\text{sqrd},2}(t)$ is in phase with $\sin(t)$. This controller can be expressed as

$$u_{4,x} = \left(\text{sgn}\left[\cos\left(\omega t + k\psi(x,y) + \frac{\pi}{4}\right)\right] + \text{sgn}\left[\sin\left(\omega t + k\psi(x,y) + \frac{\pi}{4}\right)\right]\right)\frac{2}{\pi}\sqrt{\alpha\omega}, \tag{36}$$

$$u_{4,y} = \left(\text{sgn}\left[\cos\left(\omega t + k\psi(x,y) - \frac{\pi}{4}\right)\right] + \text{sgn}\left[\sin\left(\omega t + k\psi(x,y) - \frac{\pi}{4}\right)\right]\right)\frac{2}{\pi}\sqrt{\alpha\omega}. \tag{37}$$

In this case the λ_{ij} are determined by integrals of sign functions.

For all of the controllers above, we use the same function, $\psi(x,y) = x^2 + y^2$. For each fixed i, the controllers $u_{i,x}$ and $u_{i,y}$ are orthogonal and their gains have been chosen such that $\lambda_{i_x,i_y}(t) \equiv -\frac{1}{2}$, $\lambda_{i_y,i_x}(t) \equiv \frac{1}{2}$. Thus, the same averaged system is attained for each i:

$$\dot{\bar{x}} = a_{11}\bar{x} + a_{12}\bar{y} - b_1^2 k\alpha\bar{x}, \tag{38}$$

$$\dot{\bar{y}} = a_{21}\bar{x} + a_{22}\bar{y} - b_2^2 k\alpha\bar{y}. \tag{39}$$

We simulate how the controllers stabilize the system (19), (20) with $b_i = 1$, $a_{11} = 1$, $a_{12} = 0.75$, $a_{21} = 0.5$, and $a_{22} = 2$. With these constants, the $\{a_{ij}\}$ matrix has positive real eigenvalues 2.29 and 0.71 and the system is open loop unstable. We perform the simulation with $\omega = 100$, $k = 4$, and $\alpha = 1$. The results are in Figure 1.

Remark 2 *In order to apply Theorem 1 to the examples above, such as for the square wave of period $\frac{2\pi}{\omega}$, we must expand them as their Fourier series:*

$$\begin{aligned} u_{\text{sqr}}(\omega t + \psi(x,t)) &= \frac{4}{\pi}\sum_{n\ \text{odd}}\frac{1}{n}\sin\left(n\omega t + n\psi(x,t)\right) \\ &= \frac{4}{\pi}\sum_{n\ \text{odd}}\frac{1}{n}\sin\left(n\omega t\right)\cos\left(n\psi(x,t)\right) \\ &\quad + \frac{4}{\pi}\sum_{n\ \text{odd}}\frac{1}{n}\cos\left(n\omega t\right)\sin\left(n\psi(x,t)\right). \end{aligned}$$

A less elegant, but easier to study and on-average equivalent example of such a discontinuous bounded controller is

$$u = \sqrt{\alpha\omega}u_{\text{sqr},1}(\omega t)\cos(k\psi(x,t)) - \sqrt{\alpha\omega}u_{\text{sqr},2}(\omega t)\sin(k\psi(x,t)), \tag{40}$$

where

$$u_{\text{sqr},1}(\omega t) = \text{sgn}\left[\cos(\omega t)\right], \quad u_{\text{sqr},2}(\omega t) = \text{sgn}\left[\sin(\omega t)\right]. \tag{41}$$

Although we have written $u_{\text{sqr}}(\omega t) = \text{sgn}\left[\cos(\omega t)\right]$ so that it is easy for the reader to interpret the values of the function, the digital implementation of such a function does not require the calculation of $\cos(\omega t)$ and is instead accomplished by using a combination of a resetting ramp with slope $\frac{\omega}{2\pi}$ and the $\text{sgn}(\cdot)$ function, both of which are trivially implemented with minimal resources in fixed-integer length digital logic such as that used in high speed field programmable gate arrays (FPGA), such as:

$$u_{\text{sqr}}(\omega t) = \text{sgn}\left[\text{ramp}\left(\frac{\omega}{2\pi}t\right) - \frac{1}{2}\right], \tag{42}$$

where ramp(t) ramps from 0 up to 1 in 1 second, resets to 0, and repeats.

5 Application to Inverter Switching Control

We consider a class of systems in which discontinuous, high frequency switching control is necessary by design and for which high frequency extremum seeking is especially well suited: DC to AC voltage inverters. Inverters are the basic building blocks of many electrical systems. Control methods for inverters include the application of classical PID, sliding mode, model predictive control methods [44–48], and continue to be an active area of research in power electronics. We present a simple ESCO approach which can accommodate uncertainties in the voltage input into the system and unpredictable energy use which results in time-variation of the load. This is especially important for the uncertain/time-varying characteristics of renewable energy sources such as wind and solar due to unpredictable weather.

A typical DC to AC inverter is shown in Figure 3. A DC voltage source is connected to ground across an H-bridge and the load. The H-bridge functions by closing alternating pairs (A_1 and A_2 or B_1 and B_2) of metal-oxide-semiconductor field-effect transistors (MOSFETS), transistors designed for high frequency switching. As alternate pairs of MOSFETS are activated the resulting voltage across the circuit, V_{in}, switches from positive to negative and back. Currently available power electronics MOSFETS are capable of holding off tens of thousands of volts and switching within hundreds of nanoseconds. For our application, the switching is performed at $\sim$ 8000kHz and 709V. The output of the switching H-Bridge is followed by a simple LC filter and finally an uncertain, time-varying load, $R(t)$, across which the goal is to maintain a constant amplitude sinusoidal AC voltage.

The state equations of the circuit are $V_{in} = L\frac{di_L}{dt} + V_R$,$i_L = i_C + i_R$, $i_C = C\frac{dV_R}{dt}$, $i_R = \frac{V_R}{R}$, $V_{in} = u(t) \times V_{DC}(t)$, where i_L, i_C, and i_R are the currents through the inductor, capacitor, and resistor, respectively, and $u(t)$ is the controlled H-bridge switching signal. The system dynamics can be summarized as

$$\ddot{V}_R(t) = -\frac{V_R(t)}{LC} - \frac{\dot{V}_R(t)}{R(t)C} - \frac{V_{DC}(t)}{LC}u(t). \tag{43}$$

Defining the error variables $e_1 = V_R - V_{\text{ref}}$, $\dot{e}_1 = e_2$ and choosing the control law

$$u = \sqrt{\alpha\omega}f_{\text{sqrd}}\left[\omega t + k(J(e_1, e_2) + n(t))\right], \tag{44}$$

where $J(e_1, e_2) = (e_1 + k_2 e_2)^2$, whose minimization, is equivalent to trajectory tracking and $n(t)$ is noise. The closed loop dynamics are then

$$\begin{aligned}\dot{e}_1 &= e_2 \qquad (45)\\ \dot{e}_2 &= -\frac{e_1}{LC} - \frac{e_2}{RC} - \frac{V_{\text{ref}}}{LC} - \frac{\dot{V}_{\text{ref}}}{RC} + \ddot{V}_{\text{ref}}\end{aligned}$$

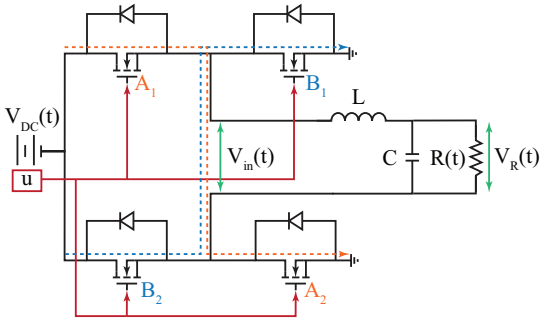

Fig. 3. The timing of the switching of the H-bridge is controlled by the control signal, $u(t)$, which closes the MOSFETS in alternating pairs, A_1 and A_2 or B_1 and B_2, causing the current to flow clockwise or counterclockwise through the circuit, respectively.

$$-\frac{V_{DC}(t)}{LC}\sqrt{\alpha\omega}f_{\text{sqrd}}\left[\omega t + kJ\left(e_1, e_2\right) + kn(t)\right]. \tag{46}$$

Theorem 1 implies that the averaged dynamics are:

$$\dot{\bar{e}}_1 = \bar{e}_2 \tag{47}$$

$$\begin{aligned}\dot{\bar{e}}_2 = &-\frac{\bar{e}_1}{LC} - \frac{\bar{e}_2}{RC} - \frac{V_{\text{ref}}}{LC} - \frac{\dot{V}_{\text{ref}}}{RC} + \ddot{V}_{\text{ref}}\\ &-\left(\frac{V_{DC}(t)}{LC}\right)^2 k\alpha k_2\left(\bar{e}_1 + k_2\bar{e}_2\right).\end{aligned} \tag{48}$$

For any $M > 0$, we can guarantee the stabilization and convergence to the origin of system (47), (48) over the compact set $e_1, r, e_2, \dot{r}, \ddot{r} \in K = \{x \in \mathbb{R} \text{ s.t. } |x| < M\}$. We do so with the Lyapunov function $V_L = \frac{e_1^2}{2} + \frac{(e_1+k_2e_2)^2}{2}$ and gains k, k_2 and α such that for all $e_1, r, e_2, \dot{r}, \ddot{r} \in K$, $\dot{V}_L < 0$.

Remark 3 *In this application, we have no choice on the magnitude of the input voltage, the only signal that the controller, u, can send is to alternate between* ± 1*, while the magnitude of the actual voltage input to the system is fixed by* $V_{\text{DC}}(t)$*:*

$$V_{\text{in}}(t) = V_{\text{DC}}(t)u(t) = V_{\text{DC}}(t)\sqrt{\alpha\omega}f_{\text{sqrd}}\left(\omega t + \dots\right). \tag{49}$$

Therefore we first choose $\omega > 0$ *and we are then forced to choose* $\alpha = \frac{1}{\omega}$*, so that the input voltage of the system satisfies the constraint:*

$$\begin{aligned}|V_{\text{in}}(t)| &= \left|V_{\text{DC}}(t)\sqrt{\alpha\omega}f_{\text{sqrd}}\left(\omega t + \dots\right)\right|\\ &= \left|V_{\text{DC}}(t)f_{\text{sqrd}}\left(\omega t + \dots\right)\right| \leq \left|V_{\text{DC}}(t)\right|.\end{aligned} \tag{50}$$

This type of constraint is exactly what the bounded form of extremum seeking presented above is especially well suited for since unknowns enter the controller dynamics as the arguments of a-priori chosen, known, bounded functions.

We demonstrate this controller by simulating a system

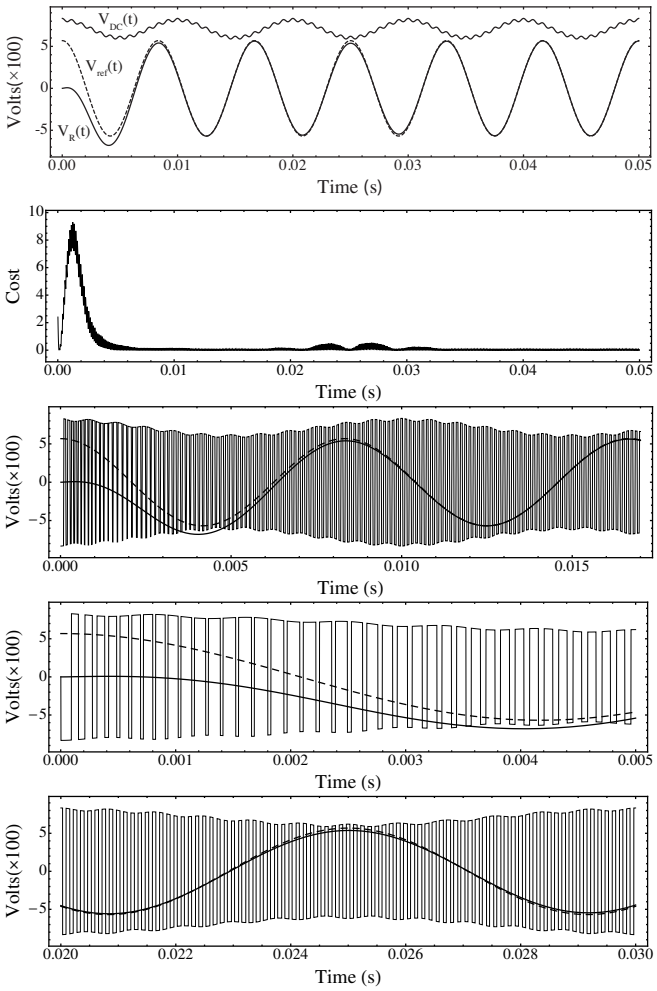

Fig. 4. The system is shown to closely track the desired output voltage trajectory despite time variation of both the DC voltage and the output load. The entire 0.05 second simulation as well as detailed views of certain time segments are shown.

with a time-varying resistance

$$R(t) = 50\left(1 + \frac{4}{5}\sin\left(2\pi \times 30t\right)\right),$$

and a two time-scale varying input voltage

$$V_{\rm DC}(t) = 709 + 106\cos\left(2\pi \times 100t\right) + 18\cos\left(2\pi \times 1200t\right).$$

The system parameters are

$$L = 3.5\text{mH},\ C = 500\mu\text{F},\ V_{\rm DC} \equiv 709V$$
$$V_{\rm ref}(t) = 570\cos\left(2\pi \times 120t\right) V.$$

Simulation results with $\omega = 2\pi \times 8000$, $\alpha = \frac{1}{\omega}$, $k = 35 \times 10^{-6}$, and $k_2 = 7.5 \times 10^{-3}$ are shown in Figure 4.

6 Conclusions

This work provides a powerful tool for the analytic design of a large class of ESCO controllers that do not require the continuity, differentiability, or periodicity of the control inputs and are immune to additive, state-independent measurement noise. We demonstrate that a large class of different dithers result in identical average system dynamics which allows a wide choice of ESCO dither type based on particular application/hardware requirements. These results are particularly useful for the design of controllers that may be simply and naturally implemented in digital circuits.

A Appendix

The proof of Theorem 1 consists of two parts, Lemma 1 and Proof 2. Lemma 1 shows that system (1), (3) converges to the average system as ω goes to infinity. Proof 2 uses the the Arzelà-Ascoli Theorem and Theorem 2 to show that when ω is sufficiently large the solutions of the original system remains close to the solutions of the average system. Before the proofs, we recall the necessary definitions and theorems.

A.1 Background

Recall that a sequence of integrable continuous functions on a compact set K is uniformly equicontinuous if for every $\epsilon > 0$, there exists a $\delta > 0$, such that: $|u_n(x) - u_m(y)| < \epsilon,\ \forall x, y \in K,$ s.t. $\|x - y\| < \delta$.

Arzelà-Ascoli Theorem [49]: If a sequence of continuous functions on a compact set is bounded and equicontinuous, then it has a uniformly convergent subsequence.

Definition 1 *Converging Trajectories Property: The systems $\dot{x} = f(t,x)$, $\dot{x} = f^\epsilon(t,x)$, with solutions $\psi(t,t_0,x_0)$ and $\psi^\epsilon(t,t_0,x_0)$, respectively, which pass through the point x_0 at time t_0, are said to satisfy the converging trajectories property if for every $\hat{T} \in (0,\infty)$ and compact set $K \subset \mathbb{R}^n$ satisfying $\{(t,t_0,x_0) \in \mathbb{R}\times\mathbb{R}\times\mathbb{R}^n : t \in [t_0, t_0+\hat{T}], x_0 \in K\} \subset \text{Dom}\psi$, for every $d \in (0,\infty)$ there exists $\epsilon^\star$ such that for all $t_0 \in \mathbb{R}$, for all $x_0 \in K$ and for all $\epsilon \in (0,\epsilon^\star)$, $\|\psi^\epsilon(t,t_0,x_0) - \psi(t,t_0,x_0)\| < d,\ \ \forall t \in [t_0, t_0+\hat{T}]$.*

With these definitions the following result of Moreau and Aeyels [33] is used in the analysis that follows.

Theorem 2 ([33]) *If the systems $\dot{x} = f(t,x)$, $\dot{x} = f^\epsilon(t,x)$ satisfy the converging trajectories property and if the origin is a GUAS equilibrium point of $\dot{x} = f(t,x)$, then the origin of $\dot{x} = f^\epsilon(t,x)$ is ϵ-Semiglobal Practical Uniform Asymptotic Stability.*

The definition of ϵ-Semiglobal Practical Uniform Asymptotic Stability is available in [33], basically it means that for any given $\delta > 0$, there exists a small enough ϵ such that the trajectory of $\dot{x} = f^{\epsilon}(t, x)$ will remain within δ of the origin.

A.2 Proof of Theorem 1

Throughout this section we assume that $\{h_{i,\omega}\}$ and $\{H_{i,\omega}\}$ are sequences of functions that satisfy the hypothesis of Theorem 1.

Lemma 1 *As* $\omega \to \infty$

$$I_1 = \int_{t_0}^{t} b_i(x_\omega, \tau) h_{i,\omega}(\tau) d\tau \to \sum_{j=1}^{m} \int_{t_0}^{t} \frac{\partial b_i(\bar{x}, \tau)}{\partial x} b_j(\bar{x}, \tau) \lambda_{j,i}(t) d\tau. \tag{A.1}$$

Proof 1 *Integrating* I_1 *by parts gives*

$$I_1 = b_i(x(\tau), \tau) H_{i,\omega}(\tau)\big|_{t_0}^{t} - \int_{t_0}^{t} \frac{db_i(x, \tau)}{d\tau} H_{i,\omega}(\tau) d\tau.$$

As $\omega \to \infty$ *the first term of* I_1 *converges uniformly to zero. The second term can be expanded as*

$$\underbrace{\int_{t_0}^{t} \frac{\partial b_i(x, \tau)}{\partial \tau} H_{i,\omega}(\tau) d\tau}_{I_{2,1}} + \underbrace{\int_{t_0}^{t} \frac{\partial b_i(x, \tau)}{\partial x} f(x, \tau) H_{i,\omega}(\tau) d\tau}_{I_{2,2}} + \sum_{j=1}^{m} \underbrace{\int_{t_0}^{t} \frac{\partial b_i(x, \tau)}{\partial x} b_j(x, \tau) h_{j,\omega}(\tau) H_{i,\omega}(\tau) d\tau}_{I_{2,3}}.$$

Since the functions $b_i(x, t)$ *are continuously differentiable, and* x *is in a compact set, the functions* $\{H_\omega\}$ *converge uniformly to zero, the terms* $I_{2,1}$ *and* $I_{2,2}$ *vanish as* $\omega \to \infty$*. The weak convergence assumption applied to* $I_{2,3}$ *give the desired conclusion.*

We now establish Theorem 1.

Proof 2 *Assume the hypothesis of Theorem 1, fix a compact set* $K \subset \mathbb{R}^n$ *and consider the following sequence of differential equations on* K

$$\dot{x}_\omega = f(x_\omega, t) + \sum_{i=1}^{m} b_i(x_\omega, t) h_{i,\omega}(t), \quad x_\omega(t_0) = x_0. \tag{A.2}$$

Because the functions f*,* b *are differentiable and* $h_{i,\omega}(t)$ *are piece-wise continuous, a unique solution of (A.2) exists [50]. For each fixed* ω *and for any* $t \geq t_0$*, the solution of (A.2) is*

$$x_\omega(t) = x_0 + \int_{t_0}^{t} f(x_\omega, \tau) d\tau + \sum_{i=1}^{m} \underbrace{\int_{t_0}^{t} b_i(x_\omega, \tau) h_{i,\omega}(\tau) d\tau}_{I_1}. \tag{A.3}$$

For any sequence $\{\omega\}$*, since we are on a compact set, the functions* $\{x_\omega\}$ *are equicontinuous and point wise bounded, therefore the Arzelà-Ascoli Theorem implies that there exists a subsequence* x_{ω_i} *that converges to* $\bar{x}$ *uniformly. To find* $\bar{x}$ *we apply Lemma 1 to* I_1 *see that the sequence* $\{x_{\omega_i}\}$ *converges to*

$$x_0 + \int_{t_0}^{t} f(\bar{x}, \tau) d\tau + \sum_{i=1}^{m} \sum_{j=1}^{m} \int_{t_0}^{t} \frac{\partial b_i(\bar{x}, \tau)}{\partial \bar{x}} b_j(\bar{x}, t) \lambda_{j,i}(t). \tag{A.4}$$

This is the solution to

$$\dot{\bar{x}} = f(\bar{x}, t) + \sum_{i,j=1}^{m} \lambda_{i,j}(t) \frac{\partial b_i(\bar{x}, t)}{\partial \bar{x}} b_j(\bar{x}, t), \quad \bar{x}(0) = x_0. \tag{A.5}$$

Because the solution is unique, these results are true for each subsequence $\{\omega_i\}$*. Because the convergence guaranteed by Arzela-Ascoly is uniform, and because this is true for any sequence* $\{\omega \to \infty\}$*, we have shown that for any* $t_0 \in \mathbb{R}$*, and any* $\delta > 0$*, there exists* $\omega^\star$ *such that for all* $\omega > \omega^\star$*, the trajectories* $x_\omega(t)$ *and* $\bar{x}(t)$ *of (A.2) and (A.5), respectively satisfy*

$$\max_{t \in [t_0, t_0 + T]} \|x(t) - \bar{x}(t)\| < \delta. \tag{A.6}$$

Therefore, the solutions of (8) and (A) satisfy the converging trajectories property for any $T \in [0, \infty)$*. Therefore, if the origin of (8) is GUAS, by Theorem 2, the origin of (A) is* $\frac{1}{\omega}$*-SPUAS. Thus, standard bootstrapping methods imply that, on* K*, if* $\lim_{t \to \infty} \|\bar{x}(t)\| = 0$*, then* $\lim_{t \to \infty} \|x_\omega(t)\| < \delta$*.*

References

[1] M. Leblanc, "Sur l'electri"cation des chemins de fer au moyen de courants alternatifs de frequence elevee," *Revue Generale de l'Electricite*, 1922.

[2] I.I. Ostrovskii, "Extremum regulation," *Automatic and Remote Control*, vol. 18, pp. 900-907, 1957.

[3] S. Morosanov, "Method of extremum control," *Automatic and Remote Control*, vol. 18, pp. 1077-1092, 1957.

[4] V. K. Obabkovm "Theory of multichannel extremal control systems with sinusoidal probe signals," *Automation and Remote Control*, vol. 28, pp. 48-54, 1967.

[5] S. Meerkov, "Asymptotic methods for investigating a class of forced states in extremal systems," *Automation and Remote Control*, vol.28, pp. 1916-1920, 1967.

[6] V. M. Volosov, "Averaging in systems of ordinary differential equations," Uspekhi matem. nauk, vol.17, No. 6, pp. 108, 1962.

[7] M. Krstić and H. Wang, "Stability of extremum seeking feedback for general dynamic systems." *Automatica,* vol. 36, pp. 595-601, 2000.

[8] Y. Tan, D. Nešić, and I. Mareels, "On non-local stability properties of extremum seeking control," *Automatica*, vol. 42, pp. 889-903, 2006.

[9] Y. Tan, D. Nešić, I. Mareels, A. Astolfi, "On global extremum seeking in the presence of local extrema," *Automatica*, vol. 45, pp. 245-251, 2009.

[10] M. Guay and T. Zhang, "Adaptive extremum seeking control of nonlinear dynamics systems with parametric uncertainties," *Automatica*, vol. 39, pp. 1283-1293, 2003.

[11] B. Srinivasan, "Real-time optimization of dynamic systems using multiple units," *International Journal of Robust and Nonlinear Control*, vol. 17, pp. 1183-1193, 2007.

[12] M. Guay, "A time-varying extremum-seeking control approach for discrete-time systems," *Journal of Process Control*, vol. 24, pp. 98-112, 2014.

[13] W. H. Moase, C. Manzie, D. Nesic, and I.M.Y. Mareels, "Extremum seeking from 1922 to 2010," in 29th *Chinese Control Conference*, 14, 2010.

[14] M.A. Rotea, Analysis of multivariable extremum seeking algorithms, Proceedings of the 2000 American Control Conference.

[15] Y. Pan, Ü. Özgünder, and T. Acarman, "Stability and performance improvement of extremum seeking control with sliding mode," *International Journal of Control*, vol. 76, pp. 968-985, 2003.

[16] L. Henning, R. Becker, G. Feuerbach, R. Muminovic, A. Brunn, W. Nitsche, R. King, "Extensions of adaptive slope-seeking for active flow control," *Journal of Systems and Control Engineering*, vol. 45 , pp. 1382-1392, 2007.

[17] K. Kim, C. Kasnakoglu, A. Serrani, M. Samimy, "Extremum-seeking control of subsonic cavity flow," *AIAA Journal*, vol. 47 pp. 195-205, 2009.

[18] O. Wiederhold, L. Neuhaus, R. King, W. Niese, L. Enghardt, B. R. Noack, M. Swoboda, "Extensions of extremum-seeking control to improve the aerodynamic performance of axial turbomachines," Proceedings of the 39th AIAA Fluid Dynamics Conference, AIAA 2009 - 4175, San Antonio, Texas, U.S.A., 2009.

[19] Y. Li, M.A. Rotea, G. Chiu, L. Mongeau, I. Paek, "Extremum seeking control of tunable thermoacoustic cooler," *IEEE Transactions on Control Systems Technology*, vol. 13, pp.527-536, 2005.

[20] J. Creaby, Y. Li, J. E. Seem, "Maximizing wind turbine energy capture using multivariable extremum seeking control," *Wind Engineering*, vol. 33, pp. 361- 387, 2009.

[21] P. Lei, Y. Li, Q. Chen, J. E. Seem, "Sequential ESC-based global MPPT control for photo- voltaic array with variable shading," *IEEE Transactions on Sustainable Energy*, vol. 2, pp. 348-358, 2011.

[22] K. Peterson, A. Stefanopoulou, "Extremum seeking control for soft landing of an electromechanical valve actuator," *Automatica*, vol. 29 pp. 1063-1069, 2004.

[23] X.T. Zhang, D.M. Dawson, W.E. Dixon, B. Xian, Extremum-seeking nonlinear controllers for a human exercise machine, IEEE/ASME Transactions on Mechatronics 11 (2006) 233-240.

[24] Y. Ou, C. Xu, E. Schuster, T.C. Luce, J.R. Ferron, M.L. Walker, D.A. Humphreys, "Design and simulation of extremum-seeking open-loop optimal control of current profile in the DIII-D tokamak," *Plasma Physics and Controlled Fusion*, vol. 50, 115001, 2008.

[25] L. Luo, E. Schuster, "Mixing enhancement in 2D magnetohydrodynamic channel flow by extremum seeking boundary control," in Proc. American Control Conf. St. Louis, MO., 2009.

[26] A. Ghaffari, M. Krstic, and S. Seshagiri, "Power optimization for photovoltaic micro-converters using multivariable Newton-based extremum seeking," *IEEE Transactions on Control Systems Technology*, vol. 22, pp. 2141-2149, 2014.

[27] S.-J. Liu and M. Krstic, "Newton-based stochastic extremum seeking," *Automatica*, vol. 50, pp. 952-961, 2014.

[28] A. Scheinker, M. Krstic, "Maximum-seeking for CLFs: Universal semiglobally stabilizing feedback under unknown control directions," *IEEE Transactions on Automatic Control,* vol. 58, pp. 1107-1122, 2013.

[29] H. Dürr, M. Stanković, C. Ebenbauer, K. Johansson, "Lie bracket approximation of extremum seeking systems," *Automatica*, vol. 49, pp. 1538 - 1552, 2013.

[30] J. Kurzweil, J. Jarnik, "Limit processes in ordinary differential equations," *Journal of Applied Mathematics and Physics*, vol. 38, pp. 241-256, 1987.

[31] H. J. Sussmann, W. Liu, "Limits of highly oscillatory controls and approximation of general paths by admissible trajectories," Proc. 30th IEEE CDC, Brighton, UK, 1991.

[32] H. J. Sussmann, "New differential geometric methods in nonholonomic path finding," Progress Systems and Control Theory, pp. 365-384, 1992.

[33] L. Moreau and D. Aeyels, "Practical stability and stabilization." *IEEE Trans. Automat. Contr.,* vol. 45, pp. 1554-1558, 2000.

[34] P.L. Kapitza, "Dynamic stability of a pendulum when its point of suspension vibrates," Soviet Phys. JETP, vol. 21, 588592, 1951.

[35] S. Meerkov, "Principle of Vibrational Control: Theory and Applications," *IEEE Transactions on Automatic Control*, vol. 14, pp. 755-762, 1980.

[36] S. Martinez, J. Cortes, F. Bullo, "Analysis and design of oscillatory control systems," *IEEE Transactions on Automatic Control*, vol.48, pp. 1164-1177, 2003.

[37] A. Scheinker, M. Bland, M. Krstic, J. Audia, "Rise-time optimization of high voltage converter modulator rise-time," *IEEE Transactions on Control Systems Technology*, vol. 22, pp. 34-43, 2013.

[38] S. Michalowsky, C. Ebenbauer, "Swinging up the Stephenson-Kapitza pendulum," Proc. 52nd IEEE CDC, Florence, Italy, 2013.

[39] H. Dürr, M. Stanković, C. Ebenbauer, K. Johansson, "Extremum seeking on submanifolds in the Euclidian space," *Automatica*, vol. 50, pp. 2591 - 2596, 2014.

[40] A. Scheinker, M. Krstic, "Non-C^2 Lie bracket averaging for non-smooth extremum seekers," *ASME Journal of Dynamic Systems, Measurement, and Control*, vol. 136, 2014.

[41] A. Scheinker, M. Krstic, "Extremum seeking with bounded update rates," *Systems & Control Letters*, vol. 63, pp. 25-31, 2014.

[42] A. Scheinker, S. Baily, D. Young, J. Kolski, M. Prokop, "In-hardware demonstration of model-independent adaptive tuning of noisy systems with arbitrary phase drift," *Nuclear Instruments and Methods in Physics Research A*, vol.756, pp.30-38, 2014.

[43] Y. Tan, D. Nesic, I. Mareels, "On the choice of dither in extremum seeking systems: a case study," *Automatica*, vol. 44, pp. 1446-1450, 2008.

[44] S. K. Chung, H. B. Shin, and H. W. Lee, "Precision control of single-phase PWM inverter using PLL compensation," *IEE Proceedings - Electrical Power Applications*, vol.152, pp. 429-436, 2005.

[45] S. Dasgupta, S. K. Sahoo, and S. K. Panda, "Single-phase inverter control techniques for interfacing renewable energy sources with micro gird - Part I: Paralle-connected inverter topology with active and reactive power flow control along with grid current shaping," *IEEE Transactions on Power Electronics*, vol. 26, pp.717-731, 2011.

[46] S. Dasgupta, S. K. Sahoo, and S. K. Panda, "Single-phase inverter control techniques for interfacing renewable energy sources with micro gird - Part II: Series-connected inverter topology to mitigate voltage-related problems along with active power flow control," *IEEE Transactions on Power Electronics*, vol. 26, pp.732-746, 2011.

[47] A. Abrishamifar, "Fixed switching frequency sliding mode control for single-phase unipolar inverters," *IEEE Transactions on Power Electronics*, vol. 27, pp. 2507-2514, 2012.

[48] S. Almer, S. Mariethoz, and M. Morari, "Dynamic phasor model predictive control of switched mode power converters," *IEEE Transactions on Control Systems Technology*, vol. 23, pp. 349-356, 2015.

[49] J. Conway. *A Course in Functional Analysis*, Springer-Verlag, New York, 1990.

[50] H. Khalil, *Nonlinear Systems*, Prentice Hall, Upper Saddle River, NJ, 2002.